ELSEVIER

Journal of Power Sources 71 (1998) 185–189

JOURNAL OF POWER SOURCES

Performance of a solid oxide fuel cell fabricated by co-firing

Himeko Ohrui*, Toshio Matsushima, Toshiro Hirai

NTT Integrated Information and Energy Systems Laboratories, 3-9-11 Midori-cho, Musashino-shi, Tokyo 180, Japan

Abstract

A solid oxide fuel cell (SOFC) was fabricated by co-firing laminated sheets of air-electrode, electrolyte, and fuel-electrode and the influence of the physical characteristics of the air-electrode on the cell performance was studied. Tailoring the sintering shrinkage of green sheets to one another was found to be an important factor in fabricating a flat and fracture-free three-layer cell. Controlling the binder content in the fuel-electrode green sheet and calcination of $La_{0.7}Sr_{0.3}MnO_3$ (LSM) powder were effective for tailoring the sintering shrinkage of green sheets. The performance of the co-fired three-layer cell was greatly influenced by the porosity of the air-electrode, and the maximum power density was attained at 70% of relative density, which is determined by the gas permeability and conductivity of air-electrode. © 1998 Elsevier Science S.A.

Keywords: Solid oxide fuel cell; Co-firing; Shrinkage; sintering characteristics; Cell performance

1. Introduction

A solid oxide fuel cell (SOFC) is an attractive system that promises high-power-generation efficiency and low emission [1]. However, the cell performance needs to be improved and production costs must be decreased to bring SOFCs into practical use. An SOFC is composed of different ceramic materials and, to date, electrochemical vapor deposition (EVD) [2], plasma spraying [3], and screen printing [4] have been used to fabricate the cell components. These procedures are complicated and need large and expensive apparatus. A simpler process that does not require a large apparatus is desired to fabricate high-performance SOFCs at low cost. Co-firing meets this requirement. In this process, the cell is fabricated by laminating air-electrode, electrolyte, and fuel-electrode green sheets, and then sintering them together at the same time.

However, co-firing has some problems to be solved. Each ceramic material shrinks at a different rate during sintering. SOFC is composed of several different ceramic materials and if the shrinkage differences are large, the co-fired sample will be warped or broken because of large interfacial stress. Thus, the sintering shrinkage of cell materials should be tailored to restrain such stress [5].

Moreover, electrodes should be porous (60–80% in relative density [6]) and electrolyte and interconnection should be dense (more than 94% in relative density [7]) for SOFC. Therefore, for a cell made by one sintering process, each cell component should have the desired configuration and warping and all damage must be prevented.

Co-firing has been applied to both tubular and flat-plate SOFCs. [8–10] Few studies on making the flat-plate SOFC have been reported because of its technical difficulties, though the flat-plate SOFC promises superior cell performance to the tubular type on account of its short current path [11]. There are two types of flat-plate cell, self-supported and supported. Takagi et al. [10] reported a self-supported cell fabricated by co-firing that was supported by a 200-μm thick electrolyte. However, the externally supported cell promises better cell performance because a thinner electrolyte (about 1/7 of the self-supported one [12]) can be fabricated. In this report, we studied the optimum conditions for co-firing on the supported cell, and successfully made three-layer cells with a 15-μm thick electrolyte. Their cell performances are also presented.

2. Experimental

2.1. Powders

In this study, 8 mol% Y_2O_3 stabilized ZrO_2 (YSZ; Tosho) and cermet of 60 wt.% NiO (Furuuchi Chemical) and YSZ were used for electrolyte and fuel-electrode, respectively.

* Corresponding author.

0378-7753/98/$19.00
PII S0378-7753(97)02758-4

For the air-electrode, a mixture of $La_{0.7}Sr_{0.3}MnO_3$ (LSM(x = 0.3)) (Seimi Chemical) and 30 wt.% YSZ was used. In order to increase the porosity of the air-electrode, spherical carbon powder with a particle size of 5 μm diameter was added to the air-electrode powder.

2.2. Specimen preparation

All specimens were fabricated using green sheets prepared by the doctor blade method. Slurries were prepared by mixing ceramic powder, binder, plasticizer, and solvent, and ball milling the mixture for 48 h. Solvent was then evaporated and slurry was tape-cast by the doctor blade method.

Specimens were prepared by laminating the green sheets and cutting them to size, and sintering. Before sintering, the binder in the specimens was burned out by heating them at 360°C.

2.3. Measurements

Sintering characteristics were evaluated by shrinkage, which was calculated based on the original length and reduced length after sintering. Relative density ξ was calculated from the measured density ρ_m which was determined from the weight and volume of the sintered body, and theoretical density ρ_{th} Of each material using Eq. (1). (The following theoretical densities of each material were used: YSZ, 5.9 g/cm^3; NiO, 6.96 g/cm^3; $La_{0.7}Sr_{0.3}MnO_3$, 6.39 g/cm^3 [13]).

$$\xi(\%) = \rho_m / \rho_{th} \times 100 \quad (1)$$

Gas permeability coefficient K was calculated by Eq. (2) using the amount of permeated gas Q and pressure difference across the specimen Δp, measurement area A, and sample thickness θ. Helium gas was used for measuring the electrolyte and fuel-electrode and nitrogen gas for the air-electrode.

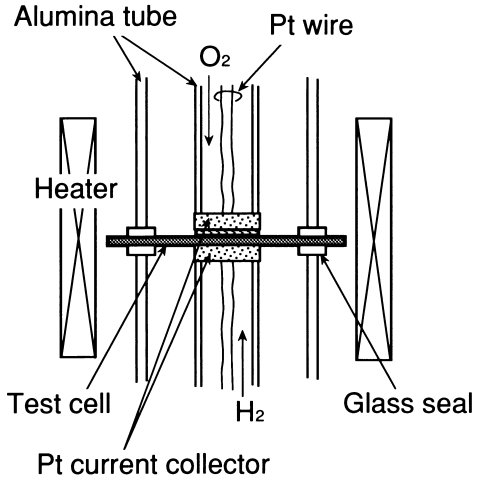

Fig. 1. Schematic diagram of the test cell fixed in the apparatus for the power generation test.

$$K\ (\mathrm{cc \cdot cm / g \cdot s}) = Q \times \theta / A \times \Delta p \quad (2)$$

Conductivity was measured by the four-terminal method at 1000°C and the microstructure of the co-fired cell was observed by scanning electron microscopy (SEM). Warp W of co-fired body was measured on a 4-cm square specimen, and calculated by Eq. (3) [14] using the length of diagonal line d, warping amount t, and sample thickness θ.

$$W(\%) = (t - \theta) / d \times 100 \quad (3)$$

Cell performance was tested on two-layer (fuel-electrode and electrolyte) and three-layer co-fired specimens (air-electrode, electrolyte, and fuel-electrode) of 30-mm diameter discs. In the case of the two-layer specimen, a 0.5 cm^2 Pt electrode was formed on the electrolyte surface by applying Pt paste. The co-fired cell was fixed in the apparatus as shown in Fig. 1. The cell performance tests were performed at 1000°C supplying pure oxygen and humidified pure hydrogen gas to each electrode at 100 cc/min.

3. Results and discussion

3.1. Selection of co-firing temperature

As described above, the electrolyte should be dense enough to prevent gas from leaking. Therefore, we selected the co-firing temperature considering electrolyte density. Fig. 2 shows the relationship between sintering temperature and relative density, and gas permeability coefficient of the electrolyte. As the sintering temperature increased, the relative density became larger and saturated at about 98% over 1300°C. As the electrolyte must have density over 94% of the theoretical one, 1300°C is an acceptable firing temperature for the electrolyte. The gas permeability coefficient decreased drastically with firing at temperatures over 1200°C. The electrolyte must have been dense enough for firing at 1300°C, because no helium gas was detected on the electrolyte fired at that temperature.

3.2. Fabrication of two-layer co-fired cell

Before making the three-layer co-fired cell, we co-fired a two-layer cell composed of fuel-electrode and electrolyte. First, after the binder had been burned out, the specimen was found to be broken and some parts of the electrolyte had peeled off. This damage is mainly related to the shrinkage difference caused in the binder burn-out process. Fig. 3 shows the influence of binder content in the green sheet on the sintering shrinkage difference between fuel-electrode and electrolyte. The shrinkage difference after binder burnout was reduced to under 2% by decreasing the binder content in the fuel-electrode green sheet. Then two layers were successfully co-fired with a relative binder content of 1. From these sintering characteristics, there was about 7% shrinkage difference between fuel-electrode and electrolyte

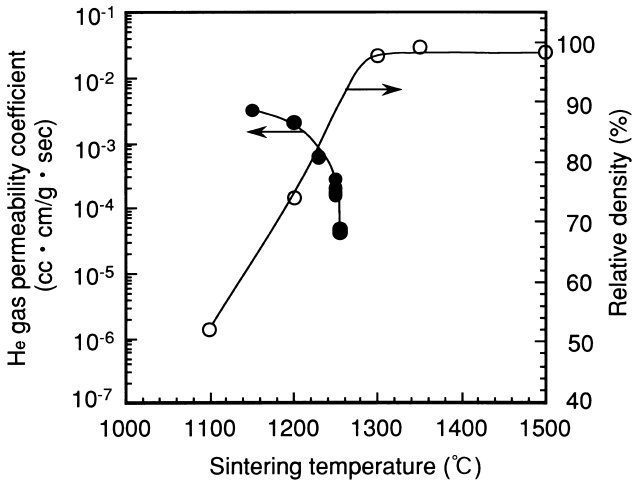

Fig. 2. Influence of the sintering temperature on the gas permeability coefficient and relative density of electrolyte.

at 1300°C but they were still co-fired successfully. This result suggests that the thickness of each layer was partly related to the co-firing process. In this co-firing study, the electrolyte was much thinner than the fuel-electrode (20 μm and 1 mm, respectively), so the interfacial stress mainly caused by shrinkage of the electrolyte was suppressed.

Fig. 4 shows the relative density of the fuel-electrode fired at each temperature. Before reduction (just after sintering), the relative density of the fuel-electrode was more than 80% for sintering over 1300°C, which is not appropriate for SOFC electrode. But under the actual power generation conditions, fuel-electrode is exposed to the H_2 and high-temperature atmosphere, and NiO is reduced to Ni. After this reduction, the relative density of the fuel-electrode decreased by 10–15%, and had porosity under 80% in the temperature tested. The relative density of the fuel-electrode fired at the co-firing temperature of 1300°C was 74%, which is porous enough for the electrode.

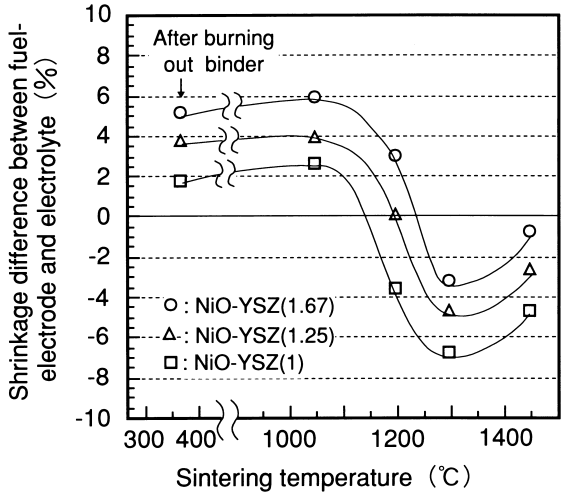

Fig. 3. Influence of the organic binder content on shrinkage. Numbers in parentheses indicate relative binder content.

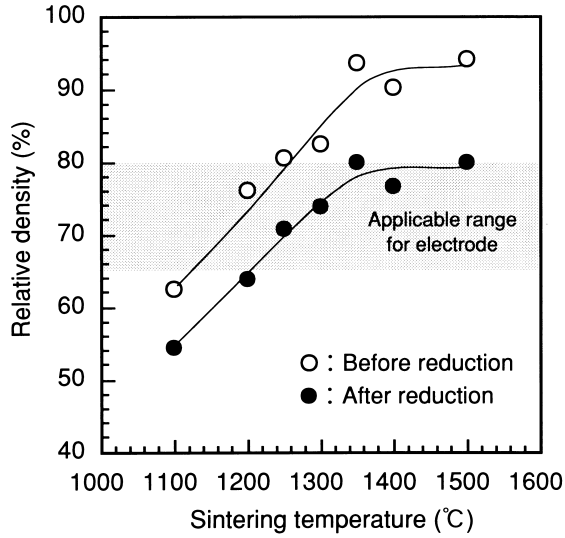

Fig. 4. Relationship between sintering temperature and relative density of fuel-electrode before and after reduction.

Fig. 5 shows the performance of the two-layer co-fired cell. The open circuit voltage (OCV) is over 1 V, which almost equals the theoretical value (1.1 V). This high OCV suggests that the electrolyte of the co-fired cell is dense enough for actual use. This two-layer co-fired cell showed superior voltage characteristics, and the maximum power density was 1.8 W/cm^2.

3.3. Fabrication of three-layer co-fired cell

For co-firing the three-layer cell, we controlled the sintering characteristics of the air electrode green sheet. Fig. 6 shows the sintering characteristics of the air-electrode and fuel-electrode green sheets. In three-layer co-firing, the stress is generated by the shrinkage difference between air-electrode and fuel-electrode, because they account for most of the thickness of the cell.

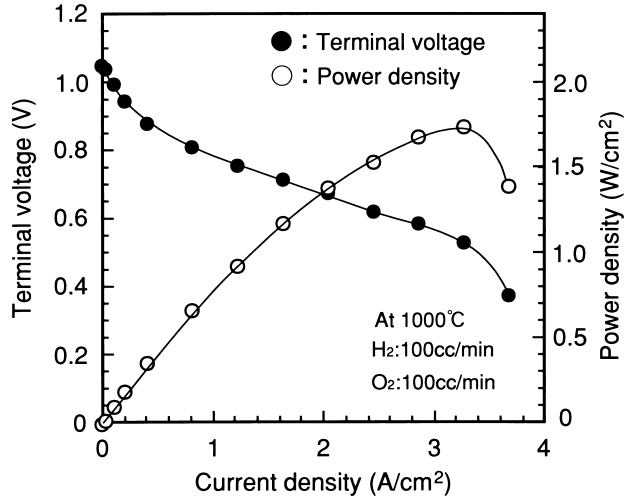

Fig. 5. *I–V* characteristics of the fuel-electrode and electrolyte of two-layer co-fired cell.

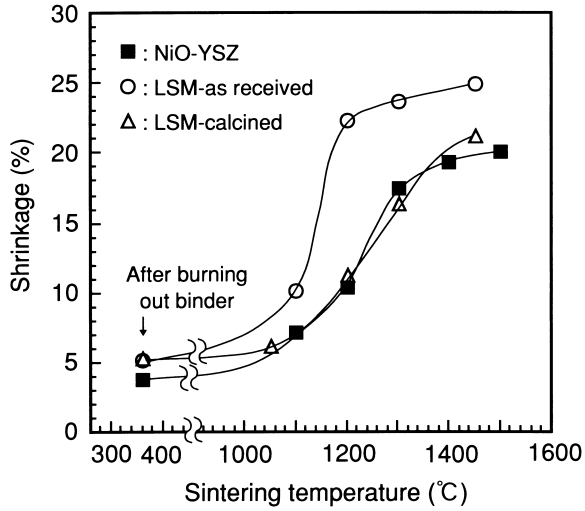

Fig. 6. Sintering characteristics of cell components. Air-electrode contains 30 wt.% YSZ.

As shown in Fig. 6, as-received LSM powder has easier sinterability. In order to co-fire three layers, the sintering characteristics of LSM powder were tailored to the fuel-electrode. Using this tailored air-electrode green sheet, a flat (warp of sintered body was under 2%) and fracture-free three-layer cell was successfully co-fired.

3.4. Improvement of air-electrode porosity

In order to clarify the influence of air-electrode porosity on cell performance, we prepared several air-electrodes having different relative densities by adding carbon powder. Fig. 7 shows the effect of carbon powder content in the green sheet on relative density and shrinkage. Relative density could be continuously decreased to 50% by raising the carbon powder content to 15 wt.%, without affecting the shrinkage changes. Thus the porosity of the air-electrode was increased from 20% to 50%. Using these

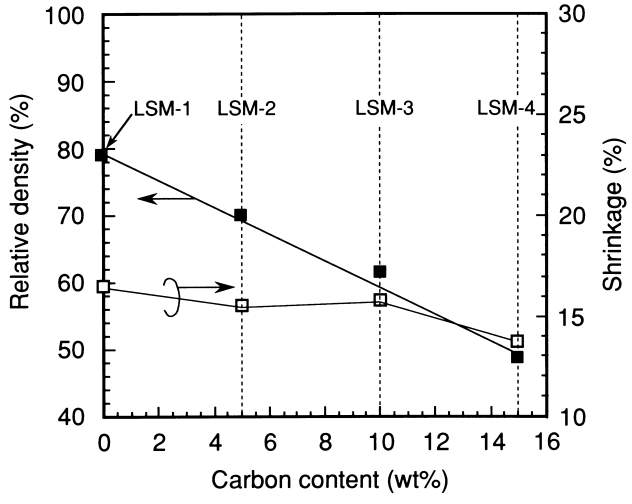

Fig. 7. Influence of carbon content on relative density and shrinkage of air-electrode. Sintering temperature was 1300°C.

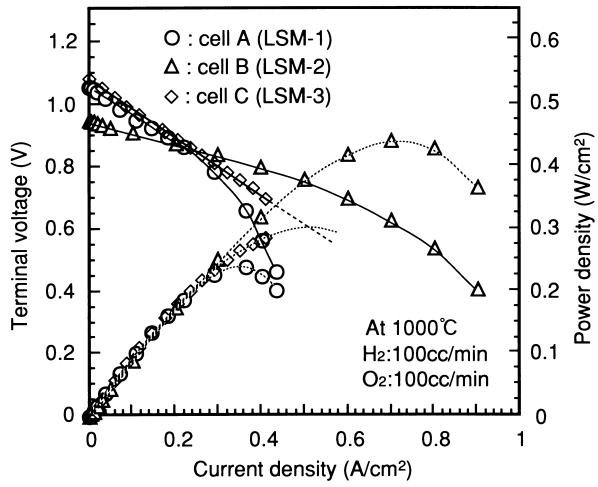

Fig. 8. Performances of three layer co-fired cells. LSM- 1, LSM-2, LSM-3 are used for the air-electrode of cells A, B and C, respectively. Solid and dotted lines indicate terminal voltage and power density, respectively.

air-electrode green sheets (LSM 1–3), three-layer cells (cells A–C) were co-fired.

Power generation tests were carried out on the co-fired cells and their characteristics are shown in Fig. 8. Cell B had the highest performance and the maximum power density was 0.45 W/cm^2. Cell C had lower performance than cell B, even though the relative density of the air-electrode was decreased. This relationship between relative density and cell performance seems to be related to the physical properties of the air-electrode. Fig. 9 shows the effect of relative density of the air-electrode on the gas permeability coefficient and conductivity of the sintered body. The gas permeability coefficient decreased but conductivity became higher with increasing relative density. Based on the highest performance being obtained with cell B, which was composed of LSM-2, we consider 70% of relative density to be acceptable from the point of view of both gas permeability and conductivity.

As described in Section 3.2, a two-layer co-fired cell of fuel-electrode and electrolyte had high power density, but

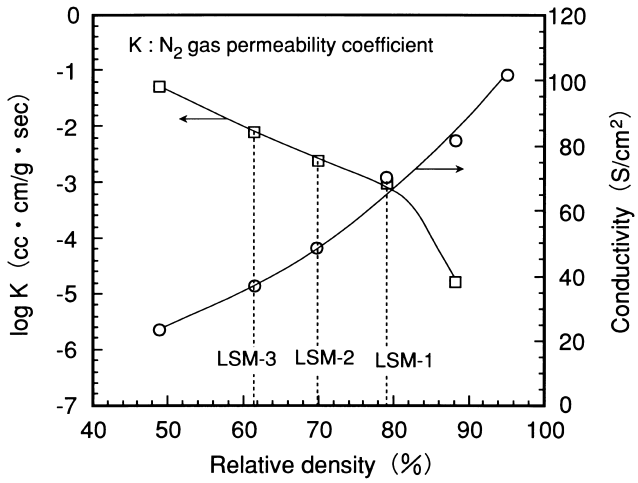

Fig. 9. Effect of relative density of air-electrode on performance.

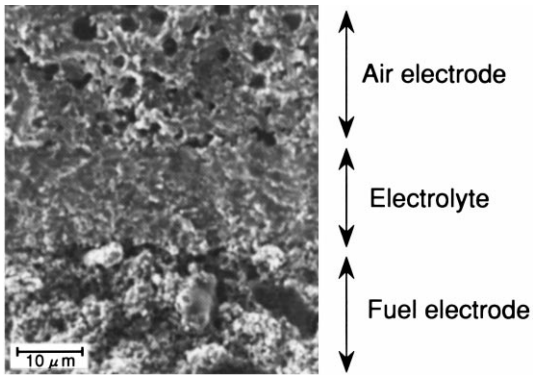

Fig. 10. Cross-sectional SEM image of three-layer co-fired cell. Air-electrode is LSM-2.

that of the three-layer cell was lower. Comparing the cell performances in Figs. 5 and 8, the slope of the I–V characteristic of the three-layer cell is steeper, so its internal resistance seems to be higher. Because cell B uses the same materials as in the two-layer co-fired cell for the fuel-electrode and electrolyte, its performance seems to be strongly affected by properties of the air-electrode. The internal resistance includes material resistance and cell reaction resistance and gas diffusion resistance in the electrode. But the gas permeability coefficients of the fuel-electrode and air-electrode fired at 1300°C are 1.87×10^{-3} and 2.66×10^{-3} cm^3.cm/g.s, respectively, and gas diffusion resistance of the air-electrode is considered to be as small as that of the fuel-electrode. Thus the internal resistance of the three-layer cell seems to be predominantly caused by the material resistance and cell reaction resistance of the air-electrode/electrolyte interface.

Fig. 10 is an SEM image of the fracture surface of co-fired cell B. The dense electrolyte about 15 μm thick is sandwiched by two porous electrodes. The effect of carbon powder addition in the green sheet is clearly observed in the air-electrode, and pores 2–5 μm in diameter remained. But the diameters of these pores are larger than those in the fuel electrode, and the length of the three-phase boundaries around the air-electrode/electrolyte interface seems to be shorter. The microstructure of the airelectrode should be improved in order to improve the performance of the co-fired cell.

4. Conclusions

Fabrication of a supported SOFC by co-firing was studied. The decrease in shrinkage difference between the fuel-electrode and electrolyte after burning out the binder was effective for co-firing the two layers. A two-layer (fuel-electrode and electrolyte) co-fired cell showed superior performance with maximum power density of 1.8 W/cm^2 being attained. This results from the thin and dense electrolyte and sufficiently porous microstructure of the fuel-electrode.

The suppression of shrinkage difference between the air-electrode and fuel-electrode was effective for the three-layer (fuel-electrode, electrolyte, and air-electrode) co-fired cell. Three-layer co-fired cells were obtained on several kinds of air-electrode with different porosities. The co-fired cell performance was mainly influenced by the porosity of the air-electrode, and maximum cell performance was 0.45 W/cm^2 at 70% of relative density, which has an acceptable gas permeability and conductivity. The performance of the co-fired three-layer cell may be further improved by optimizing the properties of the air-electrode.

References

[1] B. Riley, *J. Power Sources, 29* (1990) 223.
[2] M. Suzuki, H. Sasaki, S. Otosho, A. Kajimura, N. Sugiura and M. Ippornmatsu, *J. Electrochem. Soc., 141(7)* (1994) 1928.
[3] T. Matsushima, T. Ogata, I. Nemoto and T. Yumiba, *Trans. IEE Japan, 116-B(9)* (1996) 1060.
[4] W. Schafer, A. Koch, U. Herold-Schmidt and D. Stolten, *Solid State Ionics, 86–88* (1996) 1235.
[5] N.Q. Mihn, C.R. Horne, F. Liu, P.R. Staszak, T.L. Stillwagon and J.J. Van Ackeren, in *Proceedings of the First International Symposium on Solid Oxide Fuel Cells*, 1989, p. 307.
[6] R. Ohashi, F. Hatashi and O. Yamamoto, *Denki Kagaku, 62(9)* (1994) 797.
[7] N.Q. Minh, *J. IEE Japan, 109(10)* (1989) 826.
[8] K Eguchi, T. Setoguchi, H. Arai, R. Yamaguchi and K. Hashimoto, *Abstracts of the 33th Battery Symposium* (1992) 61.
[9] R. Okuyama and E. Nomura, *J. Ceram. Soc. Jpn., 101(9)* (1993) 1001.
[10] H. Takagi, *Zirconia Ceramics, 12* (1992) 105.
[11] N.Q. Minh, *J. Am. Ceram. Soc., 76(3)* (1993) 563.
[12] K. Murata and M. Shimotsu, *Denki Kagaku, 65(1)* (1997) 38.
[13] L.A. Tikhonova, G.I. Samal, P.P. Zhuk, A.A. Tonoyan and A.A. Vecher, *Inorg. Mater., 26* (1990) 149.
[14] *Japanese Industrial Standard* R 2203.